Quantum Electronics **38** (5) 424 – 428 (2008)

LASERS

PACS numbers: 42.55.Px; 42.60.Jf; 42.65.Re; 42.50.Nn
DOI: 10.1070/QE2008v038n05ABEH013726

Influence of superradiance on near- and far-field emission patterns in GaAs/AlGaAs heterostructures

P.P. Vasil'ev, H. Kan, T. Hiruma

***Abstract*. The near- and far-field emission patterns of GaAs/AlGaAs heterostructures are studied in the regimes of lasing and generation of femtosecond superradiant pulses. It is explicitly demonstrated that, unlike lasing, superradiant emission does not exhibit such phenomena as self-focusing, instability and deformation of near- and far-field emission patterns. The observed phenomena can be explained by the properties of the coherent cooperative electron – hole state, which has been found earlier.**

Keywords: *superradiance, near-field emission pattern, far-field emission pattern, cooperative state.*

1. Introduction

The problem of interaction of optical fields with the active medium of semiconductor lasers has attracted attention of researchers for many years. Strong nonlinearities of semiconductor media result in the appearance of different types of nonlinear optical phenomena, including self-focusing, Raman scattering, and phase conjugation [1, 2]. Most of these phenomena play a negative role in practical devices and restrict their performance. It is generally accepted that self-focusing and instability of near-field emission pattern substantially restrict fields of applications of gain-guided semiconductor lasers [3 – 5]. The lateral instability of optical field in the active region, especially in lasers with broad ($> 4 - 5$ μm) stripes, leads to the development of the filamentation of the near-field emission pattern, which in turn results in deformations and complication of the far-field emission pattern [6, 7]. To obtain spatially uniform and single-mode optical fields, structures with improved emission characteristics such as, for example, tapered waveguide lasers [8] or α-DFB lasers [9, 10] were developed.

At the same time, many experiments on the generation of femtosecond pulses in semiconductors were performed in the superradiance regime [11 – 15]. The regime of cooperative recombination in a highly nonequilibrium electron – hole system of high density ($\sim 6 \times 10^{18}$ cm^{-3}) in bulk GaAs/AlGaAs structures at room temperature was studied in these papers. It was shown that all the properties of cooperative emission can be adequately explained in terms of the collective pairing of electrons and holes, their condensation to the bottoms of the bands, and the formation of nonequilibrium coherent BCS-like state. The average lifetime of this state is 200 – 400 fs. It was also demonstrated explicitly in the experiment that at the beginning of the development of the superradiant pulse the electrons and holes undergo transitions from energy levels inside the bands down to the very bottom, i.e. to the energy levels near the band gap [13].

Note that the laser structures used in experiments were pumped by powerful current pulses with amplitudes exceeding the lasing threshold by many times. In addition, the structures did not have a built-in waveguide in the p – n junction plane. Thus, it looked like one could expect the development of the strong lateral instability of the optical beam in the active region, the emergence of filamentation and other phenomena which are typical for lasing. However, the experiments showed that this did not happen.

This work is devoted to the comparative experimental study of near- and far-field emission patterns in superradiance and lasing regimes. We will demonstrate a qualitative difference between the emission properties of superradiant pulses and standard laser emission, which has not been investigated in our experiments before.

2. Experiment

We used in the experiments GaAs/AlGaAs heterostructures with bulk (not quantum well) active region. The detailed description of them can be found elsewhere [15, 16]. The active layer consisted of pure GaAs of thickness 0.1 – 0.2 μm. The laser structures had not a built-in waveguide in the p – n junction plane. Mesa-structures of different widths were etched in the top highly doped contact p-GaAs layer to restrict the current leakage. Two types of devices were used. The first ones had active regions in the form of standard rectangular stripes of width 5 – 6 μm and length 250 – 350 μm. The other devices had tapered active layers with the width increasing along the cavity axis from 5 to 20 – 40 μm [8]. This was done to facilitate the observation of the self-focusing effect and the deformation of the optical field in the active region.

Figure 1 shows the top view of one of the laser structures with the tapered active region under test. The upper contact layer of the semiconductor structures was divided photo-

P.P. Vasil'ev P.N. Lebedev Physics Institute, Russian Academy of Sciences, Leninsky prosp. 53, 119991 Moscow, Russia;
e-mail: peter@lebedev.ru;
H. Kan, T. Hiruma Central Research Laboratory, Hamamatsu Photonics K.K., 5000 Hirakuchi, Hamamatsu City, 434-8601 Japan

Received 27 August 2007; revision received 17 January 2008
Kvantovaya Elektronika **38** (5) 424 – 428 (2008)
Translated by P.P. Vasil'ev

lithographically along the cavity axis into three sections that were electrically isolated. Two of them, including the tapered section, were optical amplifiers and were located at the cavity ends. They were pumped by 7–10-ns current pulses with the amplitude, which was varied from 500 to 800 mA. The pulse repetition rate was either 10–15 Hz or 10–40 MHz for measurements of either near- or far-field emission patterns. The central part of the laser structure was connected to a dc voltage source. A reverse dc bias up to −8 V was applied to it. This section of the laser structure was used to suppress lasing and create conditions for generation of femtosecond superradiant pulses [11, 15]. The cavity length was 350 μm.

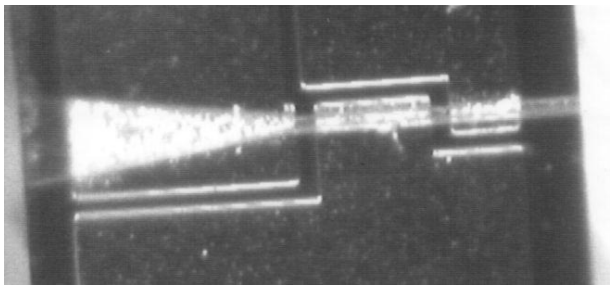

Figure 1. Microscopic view of a tapered-waveguide three-section laser structure used in the experiments.

The near- and far-field emission patterns were measured as follows. In the first case, lasers operated in the pulsed regime with a low pulse repetition rate. The edge of the active region was imaged by means of a microscopic objective with magnification by tens of times at the entrance slit of a streak camera. The ultimate time resolution of the camera at the single shot operation mode was ~ 1.5 ps. The streak image of the edge of the active region could be observed on the streak camera screen. The image on the screen was read by a CCD camera and processed in a personal computer. A detailed description of the streak camera measurements can be found in our previous paper [16]. This technique has been widely used to study spatial and spectral dynamics of emission of different semiconductor lasers for many years [1, 6].

Far-field emission patterns were measured in the pulsed regime with high repetition rates, which were required for increasing the average output power and enhancing the signal-to-noise ratio. The laser structures were fixed and spatial intensity distributions were measured by moving the photodetector (a Hioki 3664 power meter with a narrow input 1–2-mm slit aperture). The power meter was moved around the laser structure along an arc of radius ~ 14 cm.

By changing the driving conditions, it was possible to achieve different generation regimes in the laser structures, including pulsed laser generation, amplified spontaneous emission and superradiant pulses [13, 15, 16]. We studied four structures with standard narrow contacts and four structures with tapered active region. Consider, first, the effect of superradiance regime on the far-field emission of laser structures. Figure 2 presents the results related to the p–n junction plane. The data obtained for a plane perpendicular to the p–n junction plane were similar.

Figures 2a, b show the radiation power distributions for structures with a narrow rectangular contact. The solid

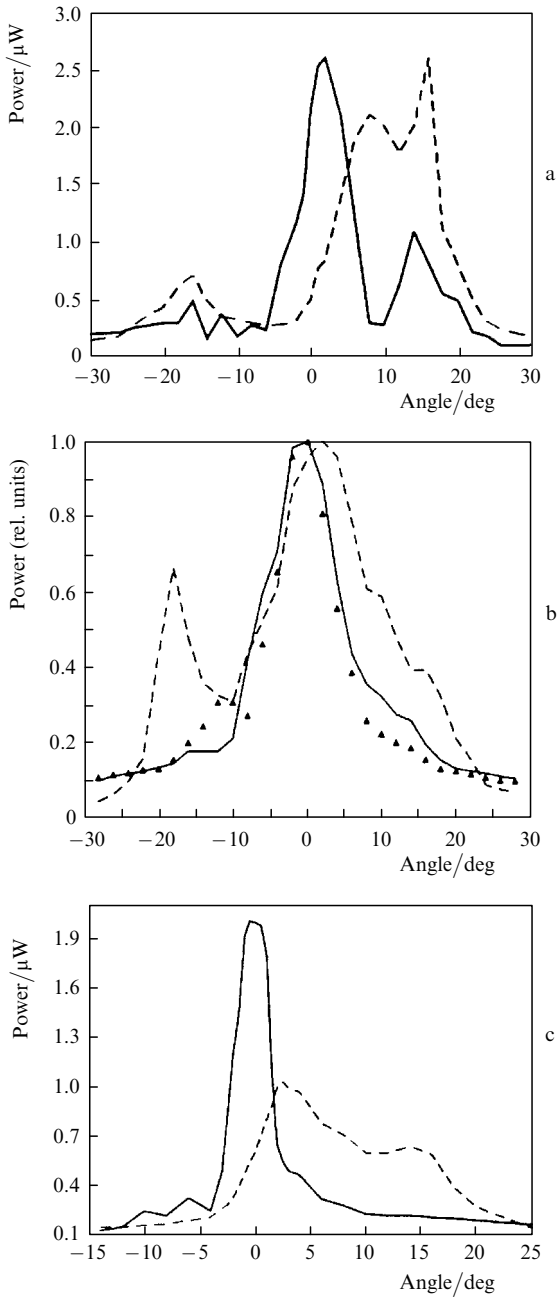

Figure 2. Far-field intensity distributions in the lasing regime (dashed curves) and in superradiance regime (solid curves) for two structures with a narrow (5–6 μm) active region (a, b) and tapered active region (c). The triangles show the far-field intensity distribution upon the uniform dc pumping (the current amplitude is 96 mA).

curves correspond to superradiance, whereas the dashed curves correspond to pulsed lasing and triangles in Fig. 2b correspond to cw lasing. In all experiments, the far-field in the superradiance regime was narrower and more symmetric than in the lasing regime. For instance, in one of the structures (Fig. 2a), the width of the far-field lobe in the superradiance regime was about 6°, whereas it was about 15° in the lasing regime. In the latter case, the centre of the radiation pattern was displaced from the axis of symmetry by no more than 10°. The pump current was the same in both cases.

The difference was even stronger for another sample with a narrow (5 μm) contact (Fig. 2b). The far-field was

detected in the lasing regime (dashed line) at the zero reverse bias and the current pulse amplitude exceeding more than five times the cw lasing threshold upon uniform current injection (80 mA). One can clearly see that the far-field is asymmetric and consists of two lobes. Its full width at half maximum (FWHM) exceeds 32°. This far-field profile implies strong self-focusing and the presence of filamentation in the active region of the laser.

By contrast, the far-field in the superradiance regime (the solid line in Fig. 2b) has only one central lobe with the FWHM $\sim 10°$. The amplitude of current pulses in the amplifying sections of the laser structure was the same, and the reverse bias across the central section was -5.9 V. Neither self-focusing nor filamentation was observed in this regime and the characteristics of the emission pattern were determined by diffraction from the structure edge and its geometry. This is confirmed by the far-field pattern in the cw lasing regime upon uniform pumping at a current of 96 mA (Fig. 2b). This current slightly exceeds the threshold of 80 mA. The emission power at such a small excess above the threshold is rather low and nonlinear optical phenomena that can cause self-focusing and instability of the optical field in the active region were insignificant.

Thus, despite a high excess of the pump over the lasing threshold, large optical power and the femtosecond duration of superradiant pulses, the far-field in the superradiance regime almost coincide with the radiation field of the structure upon cw lasing at a small excess above the threshold. This fact is confirmed by the study of the near-field emission pattern (see below).

Consider now the structures with tapered active regions. Asymmetric far-field emission patterns were observed from all the samples in the lasing regime for a large excess over the threshold current. The width of the emission pattern was much wider than the diffraction limit. The far-field pattern changed considerably with the pump current and was different in different structures. This implies the presence of the strongly developed self-focusing and instabilities of the optical field in the active region. The typical far-field pattern of one of the structures with the active region width at the output of 30 μm is presented in Fig. 2c by the dashed curve. One can see that the radiation pattern deviates from the symmetry axis by $9-10°$. It has a two-peak shape and the FWHM exceeding 16°.

The far-field pattern in the superradiance regime (the solid curve in Fig. 2c) has only one lobe with the FWHM smaller than 3°, which is more than five 5 times narrower than that in the lasing regime at the same current. Such a drastic narrowing of the far-field pattern in the regime of generation of superradiant femtosecond pulses was regularly observed for all the samples. The width of the central lobe of the radiation pattern was mainly determined by the diffraction from the structure facet and the width of the active region.

Consider now the dynamics of near-field emission patterns. The streak-camera measurements of near-field patterns are very illustrative and allow us to observe directly the instabilities of the optical flow at the structure facet, its self-focusing and filamentation. Figure 3 shows typical streak pictures of the near-field radiation in the lasing regime for the current strongly exceeding the threshold. The active region width at the output was 30 μm. Four photographs are shown at different pump currents. The instability of the optical field in time, the developed self-focusing and filamentation are clearly seen. Despite the uniform excitation of the entire active medium, the emission emerges from certain regions, its intensity changing strongly both in space and time. The pump current pulse had a rectangular shape, its duration was $4.7-5.1$ ns, the leading edge duration was 0.9 ns and the trailing edge duration was 0.5 ns.

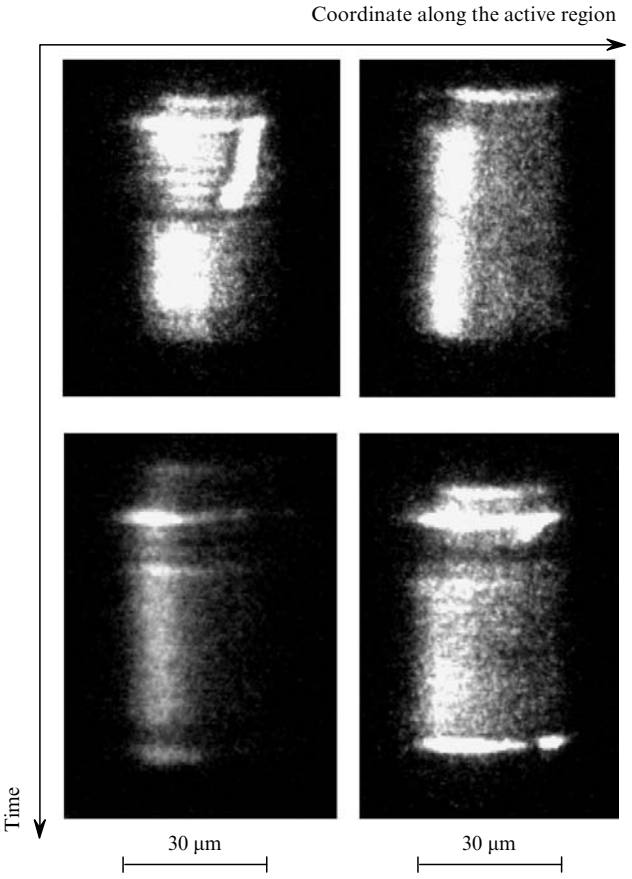

Figure 3. Near-field radiation pattern dynamics for a 30-μm-wide tapered structure in the lasing regime for driving currents of 260 and 220 mA (top) and 190 and 240 mA (bottom). The sweep duration is 2 ns.

Figure 4 shows the results obtained for a structure with a 40-μm-wide active region. The two top photographs correspond to lasing and the bottom photographs correspond to the generation of superradiant pulses. The process of filamentation and the presence of two generation channels in the active region in the lasing regime are clearly seen. By contrast, in the superradiance regime the emission is generated from the whole aperture of the active region simultaneously and is independent of pumping. Self-focusing and filamentation were never observed in any structures for any pumping in the superradiance regime. For instance, Figure 5 presents the photographs of the near-field emission dynamics in the lasing regime (top photographs) and in the superradiance regime for another structure with the tapered active region and the output aperture of 40 μm. Similarly to the previous case, self-focusing and filamentation are observed in the lasing regime. The emission emerges from restricted narrow regions, which is consistent with both experimental and theoretical results obtained in [3–6]. By contrast, the generation in the superradiance regime occurs from the entire width of the active region simultaneously.

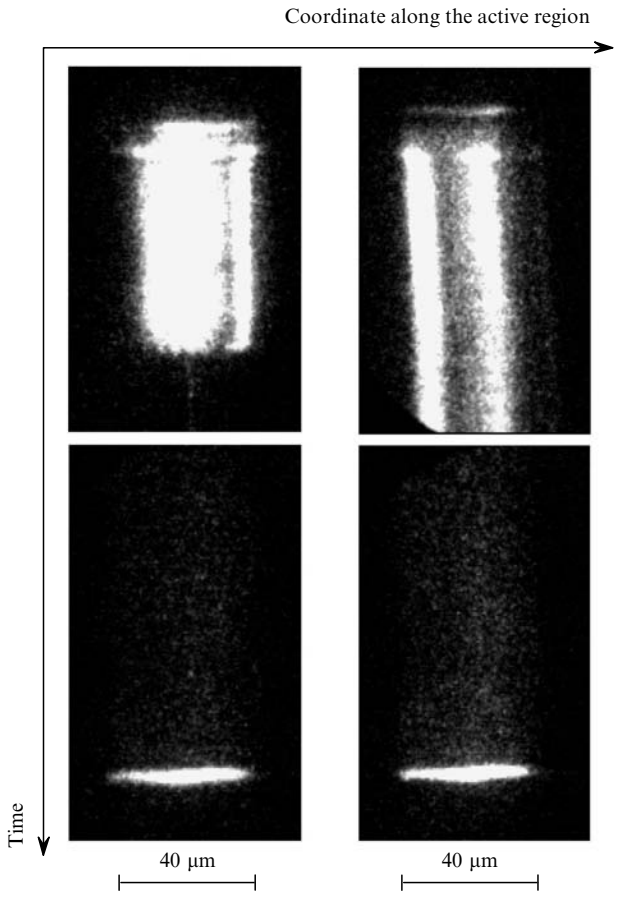

Figure 4. Near-field radiation pattern dynamics for a 40-μm-wide tapered structure in the lasing regime at currents of 260 and 240 mA (top photographs) and superradiance regime at currents of 290 and 300 mA and reverse biases −3.5 and −3.7 V (bottom photographs).

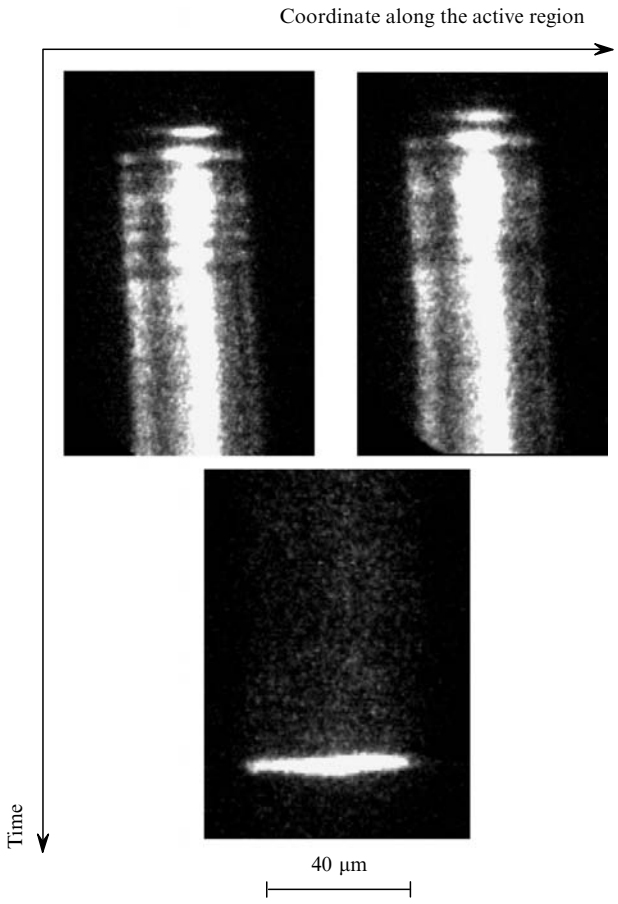

Figure 5. The same as in Fig. 4 for another 40-μm-wide tapered structure and currents of 210 and 200 mA (top) and current of 280 mA and the reverse bias of −2.9 V (bottom).

Note in conclusion of the section that we found experimentally that no deformations of the near- and far-field emission patterns occurred and self-focusing and filamentation were absent upon generation of superradiant pulses. Let us show now that this effect can be explained by the properties of the coherent cooperative electron–hole state whose radiative recombination results in the generation of superradiant pulses.

3. Discussion

The experimental results seem paradoxical at first glance. Indeed, powerful current pulses exceeding by many times the lasing threshold are applied to the structures in the superradiance regime. Self-focusing and filamentation of the emission field are observed in gain-guided lasers in the lasing regime under these conditions. In addition, the power of emitted femtosecond pulses is very high. A typical power density flux at the output of the active region of the structures can achieve 10^9 W cm^{-2} [11, 15], which is much larger than typical lasing values. Despite that, as shown in the previous section, both near- and far-field emission patterns have a right shape without any signs of filamentation, spatial instability, and self-focusing.

This can be explained as follows. It is well known [11, 17, 18] that the superradiance regime in a system of quantum oscillators consists of two temporal stages, which differ in duration strongly. First, the comparatively slow mutual phasing of the oscillators caused by the electromagnetic field occurs and a macroscopic dipole (the macroscopic polarisation of the medium) is formed. Then, the fast radiative recombination occurs and cooperative emission of a powerful and short electromagnetic pulse takes place. The superradiant pulses in semiconductors have femtosecond durations [11, 12]. If the coherent cooperative electron–hole state does form in the active medium of the laser structures, it should occupy the entire width of the pumped region. Moreover, if the collective recombination in the electron–hole system occurs, the radiation should be emitted from the entire width of the active region. This is exactly what is observed experimentally. By contrast to lasing, where the spatial coherence of the electron–hole system is absent, there are both the spatial coherency of the active medium and the coherent interaction of the medium with the optical field in case of the superradiant pulse generation [15]. Therefore, it is not strange that in all case of the superradiant pulse generation (see the bottom photographs in Figs 4 and 5) the emission emerges from the total width of the active region, although it is quite large (up to 40 μm). As a result, the far-field radiation pattern is very narrow (Fig. 2c).

4. Conclusions

We have studied the near- and far-field emission patterns of tree-section laser structures in the regimes of lasing and

generation of superradiant ultrashort pulses. Two types of the structures with narrow and tapered active regions have been investigated. All the structures were gain-guided. The samples with the tapered active region had the output aperture up to 40 μm.

It was experimentally demonstrated that both near- and far-field emission patterns were strongly different in the superradiance and standard lasing regimes. The spatial instability of the optical flux, the development of self-focusing and filamentation in the active region were observed in the latter regime. This is typical for gain-guide lasers.

By contrast, none of these effects was observed experimentally in the superradiance regime despite strong pumping of the active medium and the large emission power. Streak-camera experiments have shown that the superradiant radiation was emitted from the entire width of the active region simultaneously. As a result, the far-field radiation pattern is narrow with the FWHM of smaller than 3° for the active region width of 40 μm. The experimental results can be explained by the spatial coherence of the cooperative electron – hole state, which is formed during the generation of superradiant pulses [11 – 15].

Acknowledgements. The authors thank I.V. Smetanin for useful discussions. The work was partially supported by the Russian Foundation for Basic Research (Grant No. 06-02-16173a) and Grant No. NSh-6055.2006.2 of the Leading Research Schools.

References

1. *Nelineinaya optika poluprovodnikovykh lazerov, Trudy FIAN* (Nonlinear Optics of Semiconductor Lasers, Proceeding of FIAN), **166** (1986).
2. Vasil'ev P. *Ultrafast Diode Lasers: Fundamentals and Applications* (Norwood: Artech House, 1995).
3. Bachert H.J., Bogatov A.P., Eliseev P.G. *Kvantovaya Elektron.*, **5**, 603 (1978) [*Sov. J. Quantum Electron.*, **8**, 346 (1978)].
4. Paxton A.H., Dente G.C. *J. Appl. Phys.*, **70**, 2921 (1991).
5. Lang R.J., Mehuys D., Welch D.F., Goldberg L. *IEEE J. Quantum Electron.*, **30**, 685 (1994).
6. Gehrig E., Hess O. *IEEE J. Quantum Electron.*, **37**, 1345 (2001).
7. Bogatov A.P., Drakin A.E., Stratonnikov A.A., Konyaev V.P. *Kvantovaya Elektron.*, **30**, 401 (2000) [*Quantum Electron.*, **30**, 401 (2000)].
8. Walpole J.N. *Opt. Quantum Electron.*, **28**, 623 (1996).
9. Lang R.J., Dzurko K., Hardy A.A., Demars S., Schoenfelder A., Welch D.F. *IEEE J. Quantum Electron.*, **34**, 2196 (1998).
10. Bogatov A.P., Drakin A.E., Batrak D.V., Gunter R., Pashke K., Vencel X. *Kvantovaya Elektron.*, **36**, 745 (2006) [*Quantum Electron.*, **36**, 745 (2006)].
11. Vasil'ev P.P., Kan H., Ohta H., Hiruma T. *Zh. Eksp. Teor. Fiz.*, **120**, 1486 (2001) [*JETP*, **120**, 1486 (2001)].
12. Vasil'ev P.P. *Phys. Stat. Sol. B*, **241**, 1251 (2004).
13. Vasil'ev P.P. *Pis'ma Zh. Eksp. Teor. Fiz.*, **82**, 129 (2005) [*JETP Letters*, **82**, 129 (2005)].
14. Vasil'ev P.P., Smetanin I.V. *Phys Rev. B*, **74**, 125206 (2006).
15. Vasil'ev P.P., Kan H., Ohta H., Hiruma T. *Kvantovaya Elektron.*, **32**, 1105 (2002) [*Quantum Electron.*, **32**, 1105 (2002)].
16. Vasil'ev P.P., Kan H., Hiruma T. *Kvantovaya Elektron.*, **37**, 1001 (2007) [*Quantum Electron.*, **37**, 1001 (2007)].
17. Schuurmans M.F.H., Vrehen Q.H.F., Polder D. *Adv. Atom. Molec. Phys.*, **17**, 167 (1981).
18. Andreev A.V. *Usp. Fiz. Nauk*, **160**, 1 (1990).